Research Article

NEURAL REGENERATION RESEARCH
www.nrronline.org

Emodin attenuates inflammation and demyelination in experimental autoimmune encephalomyelitis

Yue-Ran Cui, Zhong-Qi Bu, Hai-Yang Yu, Li-Li Yan, Juan Feng*

https://doi.org/10.4103/1673-5374.358612

Date of submission: May 12, 2022

Date of decision: August 2, 2022

Date of acceptance: September 28, 2022

Date of web publication: October 24, 2022

From the Contents

Graphical Abstract

Emodin inhibits the NLRP3 signaling pathway and suppresses microglial activation in experimental autoimmune encephalomyelitis

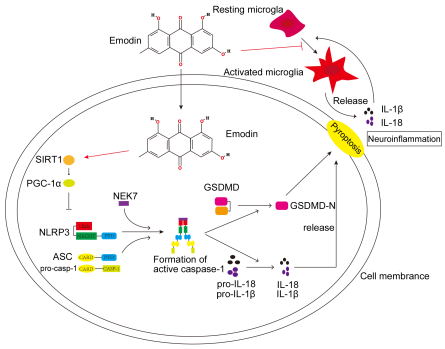

Abstract

Emodin, a substance extracted from herbs such as rhubarb, has a protective effect on the central nervous system. However, the potential therapeutic effect of emodin in the context of multiple sclerosis remains unknown. In this study, a rat model of experimental autoimmune encephalomyelitis was established by immune induction to simulate multiple sclerosis, and the rats were intraperitoneally injected with emodin (20 mg/kg/d) from the day of immune induction until they were sacrificed. In this model, the nucleotide-binding domain-like receptor family pyrin domain containing 3 (NLRP3) inflammasome and the microglia exacerbated neuroinflammation, playing an important role in the development of multiple sclerosis. In addition, silent information regulator of transcription 1 (SIRT1)/peroxisome proliferator-activated receptor-alpha coactivator (PGC-1α) was found to inhibit activation of the NLRP3 inflammasome, and SIRT1 activation reduced disease severity in experimental autoimmune encephalomyelitis. Furthermore, treatment with emodin decreased body weight loss and neurobehavioral deficits, alleviated inflammatory cell infiltration and demyelination, reduced the expression of inflammatory cytokines, inhibited microglial aggregation and activation, decreased the levels of NLRP3 signaling pathway molecules, and increased the expression of SIRT1 and PGC-1α. These findings suggest that emodin improves the symptoms of experimental autoimmune encephalomyelitis, possibly through regulating the SIRT1/PGC-1α/NLRP3 signaling pathway and inhibiting microglial inflammation. These findings provide experimental evidence for treatment of multiple sclerosis with emodin, enlarging the scope of clinical application for emodin.

Key Words: demyelination; emodin; experimental autoimmune encephalomyelitis; microglia; multiple sclerosis; neuroinflammation; NLRP3 inflammasome; PGC-1α; pyroptosis; SIRT1

Introduction

Multiple sclerosis (MS) is a demyelinating autoimmune disease of the central nervous system (CNS) (Filippi et al., 2018). MS affects more than two million people worldwide (Browne et al., 2014) and is more common in young adults. The pathological features of MS include focal demyelinating plaques in the brain, spinal cord, and optic nerve, as well as diffuse changes such as axonal injury and astrogliosis (Lassmann, 2018). Although the etiology of MS has not been fully elucidated, environmental, genetic, and epigenetic factors have been implicated in its pathogenesis (Olsson et al., 2017). Existing drugs for MS, such as interferon beta, dimethyl fumarate, and fingolimod, have strong side effects and cannot reverse the chronic progressive disabilities associated with this condition (Tintore et al., 2019; Bhargava, 2021; D'Amico et al., 2022). Therefore, there is an urgent need to develop effective and safe therapeutic drugs for MS. Experimental autoimmune encephalomyelitis (EAE) is currently the most widely used animal model of MS (Lassmann and Bradl, 2017); it partially simulates MS pathogenesis and is a useful tool for exploring the underlying molecular mechanisms of MS.

Inflammasomes are signaling complexes that sense injury and stress signals and induce inflammatory cytokine maturation and secretion. The nucleotide-binding domain-like receptor family pyrin domain containing 3 (NLRP3) inflammasome is the most widely studied inflammasome and is involved in many autoimmune and inflammatory diseases (Duewell et al., 2010; Heneka et al., 2013). NLRP3 inflammasome-related molecules are involved in MS pathogenesis, as indicated by altered levels of NLRP3 inflammasome complex components in patients with MS and in animal knockout models (Gris et al., 2010; Walsh et al., 2014; Burm et al., 2016; McKenzie et al., 2018). Inflammasome component expression is increased in the CNS tissues of MS patients. Furthermore, inflammasome activation and pyroptosis occur in human glial cells, which may affect the occurrence and development of MS. Moreover, abnormal microglial activation leads to demyelination and neurodegenerative changes (Baecher-Allan et al., 2018). Microglia, which are the intrinsic immune cells of the CNS, can exacerbate neuroinflammation by secreting chemokines, which in turn recruit immune cells to the CNS, and can also act as antigen-presenting cells to activate immune cells (Ferrari et al., 2004; Mallucci et al., 2015). In addition, microglia can be activated by pro-inflammatory cytokines such as interleukin (IL)-1β, thus creating a vicious cycle (Correale and Farez, 2015). These studies illustrate the key roles of inflammasome and microglial activation in MS. In addition, studies have demonstrated that silent information regulator of transcription 1 (SIRT1) and the downstream molecule peroxisome proliferator-activated receptor-alpha coactivator (PGC-1α) can inhibit NLRP3 inflammasome activation (Park et al., 2020; Wang et al., 2021b; Zhang et al., 2021). Research has shown that SIRT1-mediated responses are involved in a variety of physiological processes, such as oxidative stress, inflammation, and apoptosis (Yang et al., 2022). Several studies have reported the inhibitory effect of SIRT1 on the inflammatory response (Yeung et al., 2004; Planavila et al., 2011; Bai et al., 2020). These results suggest that SIRT1 can reduce neuroinflammation by inhibiting NLRP3 inflammasome activation. Moreover, related studies have found that activation

Department of Neurology, Shengjing Hospital of China Medical University, Shenyang, Liaoning Province, China
*Correspondence to: Juan Feng, MD, PhD, juanfeng@cmu.edu.cn.
https://orcid.org/0000-0002-1815-7036 (Juan Feng)

Funding: *This study was supported by the National Natural Science Foundation of China, No. 81771271; Key Research and Development Program of Liaoning Province, No. 2020JH2/10300047; and Outstanding Scientific Fund of Shengjing Hospital (all to JF).*

How to cite this article: *Cui YR, Bu ZQ, Yu HY, Yan LL, Feng J (2023) Emodin attenuates inflammation and demyelination in experimental autoimmune encephalomyelitis. Neural Regen Res 18(7):1535-1541.*

of SIRT1 can reduce the severity of EAE (Guo et al., 2021, 2022; Wang et al., 2021a). Therefore, the SIRT1/PGC-1α/NLRP3 signaling pathway may be a key pathway mediating the beneficial effects of emodin treatment on EAE.

Emodin (1, 3, 8-trihydroxy-6-methylanthraquinone; **Additional Figure 1**) is a substance extracted from traditional herbs that can alleviate the symptoms of autoimmune diseases such as ulcerative colitis and rheumatoid arthritis (Luo et al., 2018; Zhu et al., 2019). In addition, a recent study reported that emodin exhibits potent neuroprotective effects in a variety of CNS disorders such as Alzheimer's disease, Parkinson's disease, and cerebral ischemia (Mitra et al., 2022). Emodin inhibits the activity of the protein kinase casein kinase 2 (CK2). Systemic pharmacological inhibition of CK2 or knockdown of CK2b in $CD4^+$ T cells exerts neuroprotective effects in EAE (Gibson and Benveniste, 2018). Based on these studies, it seems likely that emodin would have neuroprotective effects in the context of CNS autoimmune conditions. However, there are currently no reports on the protective effects of emodin in these diseases. While a recent *in vivo* study using an EAE model reported the protective effects of emodin, the exact mechanism remains unclear (Zheng et al., 2022a). A previous study found that emodin enhances SIRT1 signaling, which in turn inhibits silica-mediated lung fibrosis (Yang et al., 2016). Another study showed that emodin inhibits NF-κB signaling and attenuates sepsis-induced lung injury through SIRT1 signaling (Liu et al., 2022a). In addition, an *in vitro* study reported that emodin decreases the level of microglia activation (Park et al., 2016). Therefore, we hypothesized that emodin may ameliorate EAE disease severity through regulation of the SIRT1/PGC-1α/NLRP3 signaling pathway and microglia. The aim of this study was to determine the role of emodin in alleviating inflammation and demyelination in an EAE rat model and its association with microglial activation and the SIRT1/PGC-1α/NLRP3 signaling pathway.

Methods

Animals

Multiple sclerosis is an autoimmune, inflammatory demyelinating disease of the CNS that is more common in women than in men (Krysko et al., 2020). Thus, basic research related to multiple sclerosis is typically carried out in female rodents (Dayani et al., 2022; Guo et al., 2022; Packialakshmi et al., 2022). We therefore used female rats to establish an EAE model. Thirty-two 6- to 8-week-old female Sprague-Dawley rats (used to establish the EAE rat model) weighing 180–200 g were purchased from the HFK Company, Beijing, China (license No. SCXK (Jing) 2019-0008). In addition, ten guinea pigs (300–350 g, used for obtaining spinal cord tissue to establish the EAE rat model) were purchased from Changsheng Company, Benxi, Liaoning, China (license No. SCXK (Liao) 2020-0001). Animals were housed in a specific pathogen-free animal laboratory and had ad libitum access to water and food. Rats and guinea pigs were maintained under a 12/12-hour light/dark cycle. The experiments were performed in accordance with the National Institutes of Health guidelines for the Care and Use of Laboratory Animals (8^{th} ed) (National Institutes of Health, 2011). This study was approved by the Medical Ethics Committee of the Shengjing Hospital of China Medical University on December 1, 2021 (approval No. 2021PS843K). Rats were randomly assigned to the following four groups (n = 8 per group): (1) control group (not immunized), (2) EAE group, (3) EAE + emodin group, and (4) emodin group (not immunized).

EAE model establishment

The EAE rat model was established as reported previously (Li et al., 2019). Briefly, after the guinea pigs were anesthetized with 2% sodium pentobarbital (0.35 mL/100 g, intraperitoneal injection, Shangyao, Shanghai, China), the spinal cords were harvested and mixed with 0.9% normal saline to make a homogenate. Incomplete Freund's adjuvant (equal volume to the homogenate, Sigma, St. Louis, MO, USA) containing Mycobacterium tuberculosis H37Ra (10 mg/mL, Difco; BD Biosciences, Franklin Lakes, NJ, USA) was added to prepare an emulsion mixture. Then, 0.4 mL of the emulsion mixture was injected rat subcutaneous into both hind footpads of the rats. The day of induction was defined as Day 0 (D0). The emulsion mixture was subcutaneously injected on D0 and D6, and pertussis toxin (Sigma) was subcutaneously injected on D0 and D2. According to our preliminary experiments and relevant studies (Pilipović et al., 2020; Dąbrowska-Bouta et al., 2021), EAE progression in this rat model is spontaneously reversible, so we sacrificed the rats at the peak of disease (on D14) before disease regression occurred. The experimental design is illustrated in **Additional Figure 2**.

Drug treatment

Emodin was purchased from Meilun, Dalian, China. The doses of emodin used were based on previous studies (Ye et al., 2019; Mei et al., 2020). The animals in the control and EAE groups received intraperitoneal injections of an equal amount (8 mL/kg) of vehicle (0.9% normal saline). The EAE + emodin and emodin groups received intraperitoneal injections of emodin at a dose of 20 mg/kg at the same time each day, starting on the day after induction of EAE (D1) and continuing until the day before sacrifice (D13). All rats were sacrificed at the peak of EAE disease, and blood samples and spinal cords were collected for subsequent procedures.

Body weight and neurobehavioral analysis

Two observers blinded to the group assignments assessed the body weights and neurological deficits of animals every morning. Neurobehavioral scores were assessed (n = 8 per group) based on a five-point scoring system (Urban et al., 1988): 0 = no signs; 1 = disappearance of tail tension, reeling gait; 2 = loss of muscle tone in both hind limbs; 3 = paralysis of hind limbs; 4 = paraplegia; and 5 = pre-death stage; ± 0.5, clinical symptoms were between the two criteria. High neurobehavioral scores indicated more severe neurological impairment and motor dysfunction.

Tissue preparation

On D14, the rats were anesthetized with 2% sodium pentobarbital (0.3 mL/100 g, intraperitoneal injection) for sample collection. The animals (n = 4 per group) used for histopathological assessment and immunohistochemistry were sacrificed, and their blood was drawn from the left cardiac ventricle via heart puncture. Next, the animals were subjected to cardiac perfusion with 0.9% normal saline and then 4% paraformaldehyde, and the lumbar enlargements of the spinal cords were harvested. The spinal cord sections were then embedded in paraffin and sliced into 5-μm thick sections. For the animals (n = 4 per group) used for polymerase chain reaction (PCR) and western blotting, blood was drawn from the left cardiac ventricle via heart puncture. Then, they were sacrificed and subjected to cardiac perfusion with 0.9% normal saline, and the lumbar enlargements of the spinal cords were harvested. The blood samples obtained were left at room temperature for 30 minutes and then centrifuged at 1200 × g for 15 minutes to obtain serum samples. All samples were stored at –80°C and used for subsequent experiments.

Histopathological assessment

To assess inflammatory cell infiltration and demyelination, spinal cord lumbar enlargement sections were subjected to hematoxylin-eosin (HE) and Luxol Fast Blue (LFB) staining. Briefly, HE staining was carried out in accordance with the manufacturer's protocol (Beyotime, Shanghai, China). For LFB staining, sections were first stained with 0.1% LFB solution (Solvent Blue 38, Sigma) at 60°C for 4 hours, then at 37°C for 4 hours, followed by differentiation. Finally, the sections were observed and images were acquired using a Nikon light microscope (Minato-ku, Tokyo, Japan). The sections were scored according to previously published criteria (Li et al., 2019): 0 = no infiltration; 1 = scattered infiltration; 2 = inflammatory cell infiltration around blood vessels; and 3 = extensive infiltration. Demyelination was scored as follows: 0 = none; 1 = focal demyelination; 2 = a few areas of demyelination; and 3 = large areas of demyelination.

Immunohistochemistry

Immunohistochemistry was performed to assess the degree of microglial aggregation and activation, using ionized calcium-binding adaptor molecule 1 (Iba-1) and CD68, respectively, as markers. After spinal cord sections were deparaffinized, hydrated, and subjected to antigen retrieval, blocking was performed using endogenous peroxidase and serum. Subsequently, the sections were incubated with anti-Iba-1 (rabbit polyclonal antibody against rat, 1:200, ProteinTech Group, Chicago, IL, USA, Cat# 10904-1-AP, RRID: AB_2224377) and anti-CD68 (mouse monoclonal antibody against rat, 1:100, Abcam, Cambridge, UK, Cat# ab31630, RRID: AB_1141557) primary antibodies overnight at 4°C (14–16 hours). Sections were incubated with biotin-labeled anti-mouse/rabbit secondary antibody (Maixin, Fuzhou, Fujian, China, Cat# KIT-9710) at 37°C for 30 minutes the following day, followed by 3,3′-diaminobenzidine staining (Cat# DAB-0031, Maixin). Finally, the sections were observed and images of the immunocomplexes were captured using a Nikon light microscope (Minato-ku, Tokyo, Japan).

Real-time PCR

On D14, all rats were anesthetized, and the lumbar enlargements of the spinal cord were harvested. RNAiso Plus (Takara, Shiga, Japan) was used to extract total RNA from the lumbar enlargements. Reverse transcription and real-time PCR were performed in accordance with the manufacturer's protocols (Vazyme, Nanjing, China). The PCR conditions were as follows: stage 1, repeats: 1, 95°C, 30 seconds; stage 2, repeats: 40, 95°C, 10 seconds, 60°C, 30 seconds; stage 3, repeats: 1, 95°C, 15 seconds, 60°C, 60 seconds, 95°C, 15 seconds. The $2^{-\Delta\Delta ct}$ method (Livak and Schmittgen, 2001), normalized to glyceraldehyde 3-phosphate dehydrogenase (*GAPDH*), was used to analyze the results. The primer sequences are listed in **Table 1**.

Table 1 | **Sequences of primers for real-time polymerase chain reaction**

Genes	Sequences
COX-2	Forward: 5'-GCA AAT CCT TGC TGT TCC AAC C-3'
	Reverse: 5'-GGA GAA GGC TTC CCA GCT TTT G-3'
iNOS	Forward: 5'-CAC CAC CCT CCT TGT TCA AC-3'
	Reverse: 5'-CAA TCC ACA ACT CGC TCC AA-3'
TNF-α	Forward: 5'-TGA ACT TCG GGG TGA TCG-3'
	Reverse: 5'-GGG CTT GTC ACT CGA GTT T-3'
IL-6	Forward: 5'-AGA AAA GAG TTG TGC AAT GGC A-3'
	Reverse: 5'-GGC AAA TTT CCT GGT TAT ATC C-3'
IL-1β	Forward: 5'-TGG CAG CTA CCT ATG TCT TGC-3'
	Reverse: 5'-CCA CTT GTT GGC TTA TGT TCT G-3'
IL-18	Forward: 5'-AAA CCC GCC TGT GTT CGA-3'
	Reverse: 5'-TCA GTC TGG TCT GGG ATT CGT-3'
GAPDH	Forward: 5'-GAC ATG CCG CCT GGA GAA AC-3'
	Reverse: 5'-AGC CCA GGA TGC CCT TTA GT-3'

COX-2: Cyclooxygenase-2; GAPDH: glyceraldehyde 3-phosphate dehydrogenase; IL-18: interleukin-18; IL-1β: interleukin-1β; IL-6: interleukin-6; iNOS: inducible nitric oxide synthase; TNF-α: tumor necrosis factor-α.

Western blot analysis

Total protein was extracted from the lumbar enlargements using radioimmunoprecipitation assay lysis buffer (Beyotime) and phenylmethanesulfonyl fluoride (Beyotime). Protein concentrations were measured using a bicinchoninic acid protein assay kit (Beyotime). Protein samples (40 μg each) were separated by electrophoresis on a 12% sodium dodecyl sulfate-polyacrylamide gel (Beyotime) and transferred to polyvinylidene fluoride membranes (Millipore, Billerica, MA, USA). Then, 5% non-fat milk was used to block the membranes at 37°C for 30 minutes. To detect the expression levels of SIRT1, PGC-1α, and NLRP3 signaling pathway components, the membranes were incubated with following primary antibodies overnight at 4°C: anti-NLRP3 (rabbit polyclonal antibody against rat, 1:1000, Abclonal, Woburn, MA, USA, Cat# A5652, RRID: AB_2766412), anti-caspase-1 (rabbit polyclonal antibody against rat, 1:1000, Abclonal, Cat# A0964, RRID: AB_2757485), anti-apoptosis associated speck-like protein containing CARD (ASC; rabbit polyclonal antibody against rat, 1:1000, Zenbio, Chengdu, China, Cat# 340097, RRID: AB_2921364), anti-SIRT1 (rabbit monoclonal antibody against rat, 1:1000, Zenbio, Cat# R25721, RRID: AB_2921365), anti-PGC-1α (rabbit polyclonal antibody against rat, 1:1000, Zenbio, Cat# 381615, RRID: AB_2921366), anti-gasdermin D N-terminal fragment (pyroptosis marker, rabbit monoclonal antibody against rat, 1:1000, CST, Danvers, MA, USA, Cat# 46451S, RRID: AB_2921367); and anti-β-actin (mouse monoclonal antibody against rat, 1:10,000, ProteinTech Group, Chicago, IL, USA, Cat# 66009-1-Ig, RRID: AB_2687938). Next, the membranes were incubated with goat anti-rabbit secondary antibodies (1:10,000, ProteinTech Group, Cat# SA00001-2, RRID: AB_2722564) and goat anti-mouse secondary antibodies (1:10,000, ProteinTech Group, Cat# SA00001-1, RRID: AB_2722565) at 37°C for 30 minutes. Enhanced chemiluminescence reagents (Tanon, Shanghai, China) were used to visualize protein expression. The results were semi-quantified using ImageJ software 1.46r (National Institutes of Health, Bethesda, MD, USA) (Schneider et al., 2012) and normalized to β-actin.

Cell culture and treatment

BV2 microglial cells (Cat# CL-0493, RRID: CVCL-0182) were purchased from Procell, Wuhan, Hubei, China, and their identity was confirmed by short tandem repeat analysis. Cells were cultured in Dulbecco's modified Eagle medium/high glucose (KeyGENE, Nanjing, Jiangsu, China) supplemented with 10% fetal bovine serum (Lonsera, Canelones, Uruguay) and 1% penicillin/streptomycin solution (Procell) at 37°C and 5% CO_2 (humidified atmosphere). Lipopolysaccharide (LPS; 1 μg/mL, Sigma) and adenosine triphosphate (ATP; 5 mM, MCE, Shanghai, China) were used to activate BV2 cells as previously described (Liu et al., 2021b). The cells were divided into the following three groups for the *in vitro* experiments: (1) control group (no treatment); (2) model group (treated with LPS for 3 hours followed by ATP for 30 minutes); and (3) treatment group (emodin pretreatment for 24 hours followed by LPS + ATP treatment). The experimental design is illustrated in **Additional Figure 3**.

Cell viability detection

The effect of emodin on BV2 cell viability was assessed to determine the appropriate concentration of emodin for use in subsequent experiments. We used a cell counting kit-8 assay (APExBIO, Houston, TX, USA) to detect cell viability. Briefly, cells were seeded into 96-well plates at a density of 7×10^3 per well and incubated for 24 hours. The cells were then treated with different concentrations of emodin (0, 5, 10, 25, 50, 100 μM) for 24 hours, after which 10 μL of cell counting kit-8 solution was added to each well, and the plates were incubated for 2 hours at 37°C in the dark. Absorbance was then measured at 450 nm using a microplate reader (BioTek, Winooski, VT, USA).

Lactate dehydrogenase analysis

To assess cell pyroptosis (Jia et al., 2019; Liu et al., 2019; Wang et al., 2022a), lactate dehydrogenase (LDH) activity in serum and cell culture supernatants was detected using an LDH testing kit (Jiancheng, Nanjing, China) according to the manufacturer's protocol. Cell culture supernatants were collected and centrifuged at 900 × *g* for 20 minutes, and the centrifuged supernatants were stored at –80°C and used for subsequent experiments.

Enzyme-linked immunoassay

Serum samples and cell culture supernatants were obtained to evaluate the levels of inflammation-related cytokines. Enzyme-linked immunoassay (ELISA) kits (Meilian, Shanghai, China) were used in accordance with the manufacturer's protocol. The results were obtained by measuring the absorbance at 450 nm using a microplate reader. The concentrations were quantified by comparison to a standard curve. The antibodies and the linear dynamic range of the standard curve used for ELISA quantifications are shown in **Additional Table 1**.

Nitrite oxide detection

Nitric oxide (NO) reacts with O_2 and H_2O to generate nitrite. The concentration of NO in serum and cell culture supernatants was indirectly measured by detecting the nitrite content using colorimetric NO testing kits (serum: Jiancheng; cell culture supernatants: Beyotime) according to the manufacturers' instructions.

Statistical analysis

We used the resource equation approach described previously (Arifin and Zahiruddin, 2017) to calculate the optimal sample size, which was 4–6 rats per group. Considering that each rat can only be used for histochemistry or western blotting, and based on a previous animal study (Liu et al., 2019), we chose to include 8 rats in each group. No animals or data points were excluded from the analysis. The evaluators were blinded to the assignments. Data are presented as mean ± standard deviation (SD). GraphPad Prism 7.00 (GraphPad Software, San Diego, CA, USA, www.graphpad.com) was used for statistical analysis. All data were evaluated using one-way analysis of variance followed by Tukey's multiple comparison test. Statistical significance was set at $P < 0.05$.

Results

Effects of emodin on EAE rat body weight and neurobehavior

Decreased body weight and increased neurobehavioral scores indicate an increase in EAE severity. We recorded body weights and neurobehavioral scores from D0 to D14 (**Figure 1**). The body weights of all groups decreased from D0 to D3 and then began to increase (**Figure 1A**). From D10, the body weights of the control and emodin groups continued to increase, whereas the body weights of the EAE and EAE + emodin groups began to decrease. The body weights of the EAE + emodin group were between those of the control and EAE groups. There was a significant difference in body weights between the EAE + emodin and EAE groups from D4 onwards, suggesting that emodin can alleviate body weight loss in EAE rats. Both the EAE + emodin and EAE groups exhibited onset of disease symptoms on D9 and reached the peak of disease at D14, indicating that emodin did not delay the onset of EAE (**Figure 1B**). From D10, the neurobehavioral scores of the EAE + emodin group were decreased compared with those of the EAE group, implying that emodin alleviated neurobehavioral deficits in EAE rats.

Effects of emodin on histopathological changes in EAE rats

EAE rats were sacrificed on D14 (the peak of the disease) for HE and LFB staining to assess histopathological changes in the spinal cord (**Figure 1C** and **D**). HE staining of the lumbar enlargement of the spinal cord revealed clear inflammatory cell infiltration in EAE rats, while the degree of infiltration in the EAE + emodin group was markedly reduced (**Figure 1C** and **E**). LFB staining of the lumbar enlargement of the spinal cord showed that the degree of demyelination in the EAE + emodin group was markedly reduced compared with that in the EAE group (**Figure 1D** and **F**). Collectively, these results demonstrate that emodin alleviated inflammatory cell infiltration and demyelination in an EAE rat model.

Effects of emodin on inflammatory cytokine expression in the lumbar enlargements of EAE rats

To evaluate the effects of emodin on the degree of inflammation in EAE rats, we performed real-time PCR, ELISA, and NO detection; the results from these analyses are shown in **Figure 2**, respectively. We found a marked increase in the level of inflammation in EAE rats, while emodin markedly reduced the degree of inflammation.

Effects of emodin on microglial aggregation and activation in the lumbar enlargements of EAE rats

Iba-1 and CD68 levels in the lumbar enlargement of the spinal cord were assessed by immunohistochemistry. Iba-1 is mainly expressed in macrophages and reflects the degree of microglial aggregation. CD68 plays a role in the phagocytic activity of tissue macrophages and indicates the microglial M1 phenotype and degree of microglial activation (Brown and Neher, 2010). We observed a clear increase in Iba-1 and CD68 levels in the EAE group compared with those in the control group, whereas treatment with emodin inhibited this increase (**Figure 3A** and **B**).

We next performed a series of *in vitro* experiments to further investigate the effect of emodin on microglial activation. The results of the cell counting kit-8 assay showed a concentration-dependent effect of emodin on BV2 cell viability: cell viability increased with treatment with up to 50 μM emodin and decreased at concentrations greater than 50 μM (**Figure 3C**). LDH analysis demonstrated that emodin (25 μM) markedly attenuated LDH activity in cell culture supernatants from BV2 cells induced with LPS + ATP (**Figure 3D**). In subsequent experiments, 25 μM emodin was used as the standard treatment concentration. Follow-up ELISA and NO assays showed a marked decrease in the activation of pro-inflammatory factors (tumor necrosis factor (TNF)-α, and NO) in BV2 cells pretreated with emodin (**Figure 3E** and **F**) and a clear increase in the expression of anti-inflammatory cytokines (interleukin (IL)-10, and arginase-1) (**Figure 3G** and **H**). These findings suggest that emodin can inhibit microglial activation.

Effects of emodin on the NLRP3 signaling pathway in the lumbar enlargements of EAE rats

Our results suggested that emodin alleviates disease severity in EAE rats, potentially through the NLRP3 signaling pathway. Thus, western blotting was carried out to assess the level of NLRP3-related molecules in the lumbar enlargement of the spinal cord (**Figure 4A**). We observed a markedly higher level of related molecules in the EAE group than in control group, and treatment with emodin markedly reduced the expression of these molecules (**Figure 4B–D**). Next, we assessed the expression levels of IL-1β and IL-18, two key inflammatory cytokines that function as downstream effectors of the NLRP3 signaling pathway. Real-time PCR analysis showed that the mRNA levels of IL-1β and IL-18 in the lumbar enlargement were clearly higher in EAE rats than in the control group (**Figure 4E**). ELISA analysis yielded similar results at the protein level (**Figure 4F**). However, treatment with emodin markedly attenuated IL-1β and IL-18 expression levels (**Figure 4E** and **F**). As a control, we treated healthy rats with emodin and found that emodin did not markedly affect clinical signs, histopathology, the expression of inflammatory cytokines, microglial aggregation and activation, or the NLRP3 signaling pathway in healthy rats.

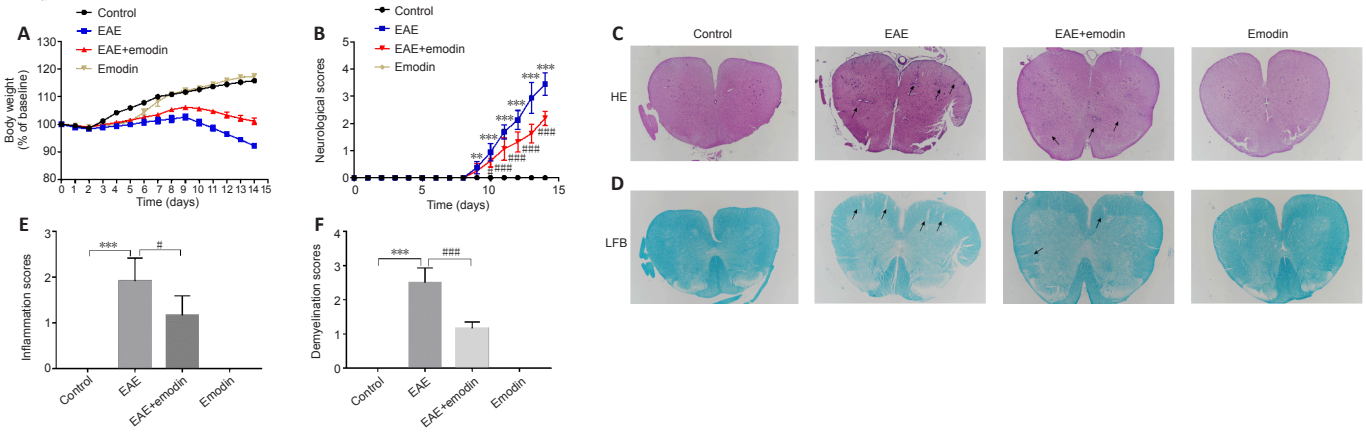

Figure 1 | **Emodin alleviates the clinical signs and degree of inflammation and demyelination of experimental autoimmune encephalomyelitis rats.**
(A) Body weights were recorded from D0 to D14 (n = 8). (B) Neurobehavioral scores were recorded from D0 to D14 (n = 8). (C, D) HE and LFB staining were used to assess the degree of inflammatory cell infiltration and demyelination, respectively (n = 4, original magnification 40×). Lesions are indicated with black arrows. (E, F) Inflammation (HE staining) and demyelination (LFB staining) scores. Treatment with emodin decreased inflammation and demyelination in the EAE rats. All data are presented as mean ± SD. $^{**}P < 0.01$, $^{***}P < 0.001$, *vs.* control group; $^{\#}P < 0.05$, $^{\#\#\#}P < 0.001$, *vs.* EAE group (one-way analysis of variance followed by Tukey's multiple comparison test). EAE: Experimental autoimmune encephalomyelitis; HE: hematoxylin-eosin; LFB: Luxol Fast Blue.

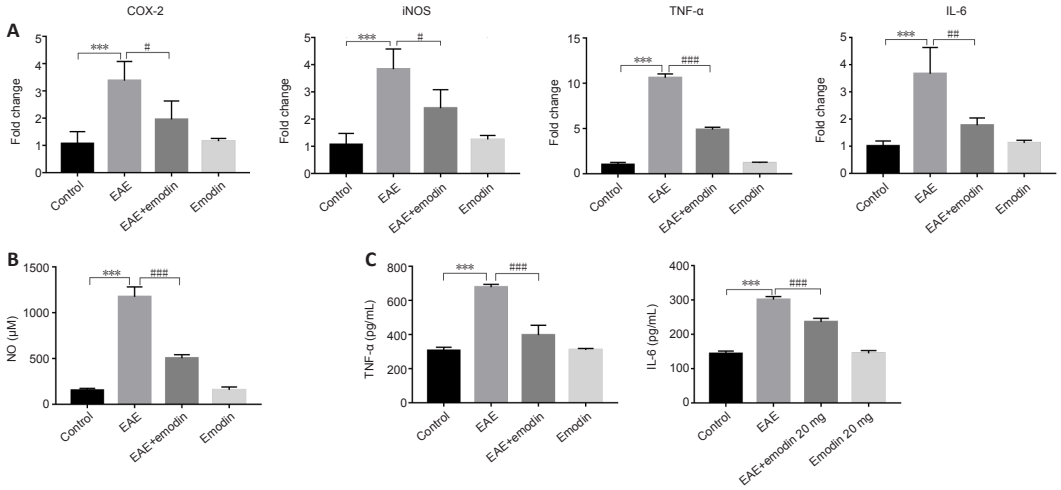

Figure 2 | **Emodin decreases inflammatory cytokine levels in the lumbar enlargements of experimental autoimmune encephalomyelitis rats.**
(A) Real-time PCR was used to assess the mRNA levels of inflammatory cytokines in the lumbar enlargement (n = 4). (B) Serum NO levels (n = 8). (C) ELISA was used to detect the serum levels of inflammatory cytokines (n = 8). All data are presented as mean ± SD. $^{**}P < 0.01$, $^{***}P < 0.001$, *vs.* control group; $^{\#}P < 0.05$, $^{\#\#}P < 0.01$, $^{\#\#\#}P < 0.001$, *vs.* EAE group (one-way analysis of variance followed by Tukey's multiple comparison test). COX-2: Cyclooxygenase-2; EAE: experimental autoimmune encephalomyelitis; ELISA: enzyme-linked immunoassay; IL-6: interleukin-6; iNOS: inducible nitric oxide synthase; NO: nitric oxide; PCR: polymerase chain reaction; TNF-α: tumor necrosis factor-α.

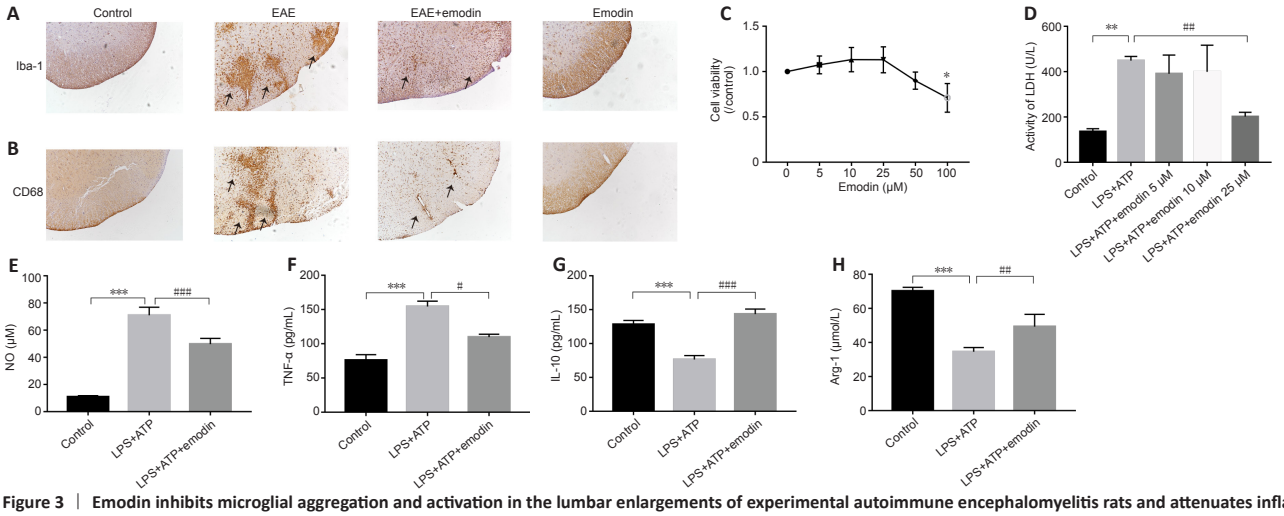

Figure 3 | **Emodin inhibits microglial aggregation and activation in the lumbar enlargements of experimental autoimmune encephalomyelitis rats and attenuates inflammation in BV2 cells.**
(A, B) The immunohistochemistry results showed that the extent of microglial aggregation (Iba-1-positive; A) and activation (CD68-positive; B) was higher in the EAE group than in the control group and lower in the EAE + emodin group than in the EAE group (original magnification 40×). (C) Viability of emodin-treated BV2 cells as detected by CCK-8 assay. (D) LDH activity. (E) NO levels. (F–H) ELISA was used to detect cytokine levels. All data are presented as mean ± SD. The experiment was repeated four (A, B) or three (C–H) times. $^{*}P < 0.05$, $^{**}P < 0.01$, $^{***}P < 0.001$, *vs.* control group; $^{\#}P < 0.05$, $^{\#\#}P < 0.01$, $^{\#\#\#}P < 0.001$, *vs.* LPS + ATP group (one-way analysis of variance followed by Tukey's multiple comparison test). Arg-1: Arginase-1; ATP: adenosine triphosphate; CCK-8: cell counting kit-8; EAE: experimental autoimmune encephalomyelitis; ELISA: enzyme-linked immunoassay; Iba-1: ionized calcium-binding adaptor molecule 1; IL-10: interleukin-10; LDH: lactate dehydrogenase; LPS: lipopolysaccharide; NO: nitric oxide; TNF-α: tumor necrosis factor-α.

Effects of emodin on pyroptosis in the lumbar enlargements of EAE rats

Pyroptosis is involved in EAE pathogenesis (Govindarajan et al., 2020). To assess the effects of emodin on pyroptosis in EAE rats, we performed LDH and western blotting assays. LDH activity was markedly higher in serum from EAE rats than that from controls, but was markedly lower in the EAE + emodin group than in the EAE group (**Figure 5A**), which suggests that emodin can alleviate the degree of cell damage. Western blotting detection of the level of the gasdermin D N-terminal fragment in the lumbar enlargement of the spinal cord yielded similar results (**Figure 5B**). Collectively, these results indicated that emodin reduced the degree of pyroptosis in EAE rats. Moreover, emodin did not markedly affect pyroptosis in healthy rats.

Effects of emodin on SIRT1/PGC-1α expression in the lumbar enlargements of EAE rats

SIRT1 and PGC-1α are associated with the NLRP3 inflammasome and participate in a variety of inflammatory diseases (Tang et al., 2017; Xia et al., 2021). We therefore detected SIRT1 and PGC-1α expression levels in the lumbar enlargement (**Figure 5C**). SIRT1 and PGC-1α levels were clearly lower in EAE rats than in controls, and markedly higher in the EAE + emodin group compared with those in the EAE group. However, SIRT1 expression in the lumbar enlargement of healthy rats treated with emodin was 1.3 times higher than in the control group.

Discussion

In this study, we established an EAE rat model and investigated the effects of emodin on inflammation and demyelination, as well as the underlying molecular mechanism. The results demonstrated that emodin can alleviate the clinical signs and the degree of inflammation and demyelination in EAE rats. In addition, we found that the therapeutic effects of emodin in EAE rats may be related to the inhibition of NLRP3 inflammasome activation. Furthermore, SIRT1 and PGC-1α expression level were higher in the EAE + emodin group than in the EAE group, which suggests the possible involvement of SIRT1 and PGC-1α in the inhibition of NLRP3 inflammasome activation. Moreover, our findings revealed that emodin can inhibit microglial aggregation and activation in EAE rats and attenuate inflammation in BV2 cells, thus exerting neuroprotective effects. Taken together, our results demonstrate the therapeutic effects of emodin in EAE rats and suggest that emodin may be a promising drug for the clinical treatment of MS in the future.

MS is an autoimmune disease of the CNS that mainly affects young adults (Kobelt et al., 2017; Filippi et al., 2018). Emerging evidence has implicated several pathophysiological processes in MS, such as apoptosis (Mohamed et al., 2022), autophagy (Berglund et al., 2020), and pyroptosis (Govindarajan et al., 2020). Recent studies have described the role of NLRP3 inflammasome in the pathogenesis of MS and shown that overactivation of the NLRP3 inflammasome can aggravate disease severity (Walsh et al., 2014; Burm et al., 2016). Another study found that manoalide suppresses NLRP3 inflammasome activation and alleviates EAE symptoms (Li et al., 2022). Consistent with these studies, we found that the expression levels of NLRP3 signaling pathway components were higher in the EAE group than in the control group. These findings suggest that targeting the NLRP3 signaling pathway may be a potent therapeutic approach to treating MS patients.

Emodin is derived from a variety of natural plants such as rhubarb (Huang et al., 2020). Studies have demonstrated that emodin has various pharmacological effects, such as antioxidant, immunomodulatory, and anticancer effects (Zheng et al., 2021), involving autophagy, apoptosis, and pyroptosis (Gao et al., 2022; Liu et al., 2022b). Moreover, emodin has been shown to have neuroprotective effects in the CNS. For example, emodin was reported to alleviate hyperhomocysteinemia-induced dementia (Zeng et al., 2019). In addition, emodin exerts neuroprotective effects in SH-SY5Y cells by alleviating synaptic damage and oxidative stress (Lai et al., 2020). To date, no studies have reported the clinical application of emodin in MS. A recent study found that emodin inhibited inflammation in a mouse model of EAE, thereby reducing symptoms in mice (Zheng et al., 2022a). Nevertheless, the underlying molecular mechanism is not clear, and the potential therapeutic effects of emodin in EAE rats have not been explored. Our study aimed to investigate the potential therapeutic benefit of emodin in EAE rats and the underlying

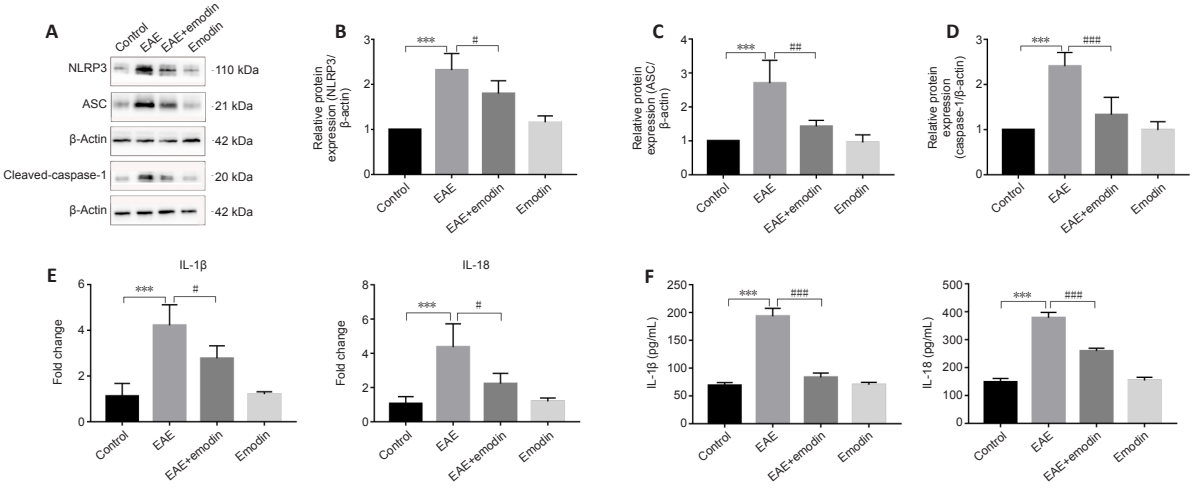

Figure 4 | **Emodin inhibits the expression of NLRP3 signaling pathway components in the lumbar enlargements of experimental autoimmune encephalomyelitis rats.**

(A–D) Western blotting was performed to detect the levels of NLRP3, ASC, caspase-1 (cleaved), and β-actin. (A) Representative image of a western blot showing bands for NLRP3, ASC, caspase-1 (cleaved), and β-actin. (B–D) Relative optical density was normalized to β-actin (n = 4). (E) Real-time polymerase chain reaction was used to detect the mRNA levels of IL-1β and IL-18 in the lumbar enlargements, and expression was normalized to GAPDH (n = 4). (F) Enzyme-linked immunoassay was performed to detect the serum levels of IL-1β and IL-18 (n = 8). All data are presented as means ± SD. ***P < 0.001, *vs*. control group; #P < 0.05, ##P < 0.01, ###P < 0.001, *vs*. EAE group (one-way analysis of variance followed by Tukey's multiple comparison test). ASC: Apoptosis associated speck-like protein containing CARD; C: control; EAE: experimental autoimmune encephalomyelitis; NLRP3: nucleotide-binding domain-like receptor family pyrin domain containing 3.

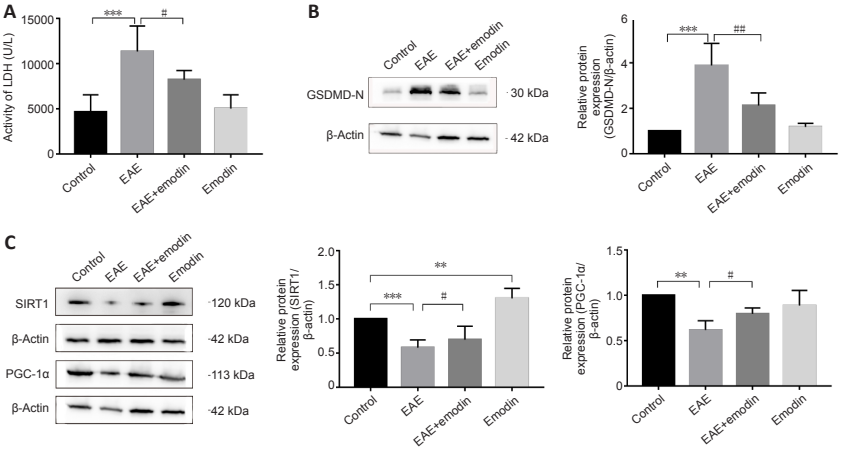

Figure 5 | **Emodin alleviates pyroptosis and SIRT1/PGC-1α expression in the lumbar enlargements of experimental autoimmune encephalomyelitis rats.**

(A) LDH analysis was performed to detect LDH activity (n = 8). (B) Representative image of western blot bands for GSDMD-N and β-actin, and relative optical density was normalized to β-actin (n = 4). (C) Representative image of western blot bands for SIRT1, PGC-1α, and β-actin, and relative optical density was normalized to β-actin (n = 4). All data are presented as means ± SD. **P < 0.01, ***P < 0.001, *vs*. control group; #P < 0.05, ##P < 0.01, *vs*. EAE group (one-way analysis of variance followed by Tukey's multiple comparison test). EAE: Experimental autoimmune encephalomyelitis; GAPDH: glyceraldehyde 3-phosphate dehydrogenase; IL-18: interleukin-18; IL-1β: interleukin-1β; LDH: lactate dehydrogenase.

molecular mechanism. The results demonstrated that EAE severity was alleviated after treated with emodin; furthermore, the expression levels of NLRP3 signaling pathway components were lower in the EAE + emodin group than in the EAE group. These inhibitory effects of emodin on NLRP3 signaling pathway are consistent with those seen in previous studies (Liu et al., 2022b; Shen et al., 2022). In addition, the expression levels of pro-inflammatory cytokines such as cyclooxygenase (COX)-2, TNF-α, and IL-6 were lower in the EAE + emodin group than in the EAE group. COX-2 is released by immune cells, its increased expression can, in part, indicate activation of immune cells and elevated levels of inflammation, and several studies have shown that it plays an important role in the inflammatory response (Barnett et al., 1994; Kim et al., 2005). It has been shown that activation of inflammasomes can lead to increased expression of COX-2 (Zhang et al., 2022). TNF-α and IL-6 are also released by immune cells, and an increase in their expression occurs as a consequence of immune cell activation and serves as an indication of elevated levels of inflammation. Inflammasome activation has been found to increase the expression levels of TNF-α and IL-6 (Latz et al., 2013); thus, these molecules are used as markers of altered inflammation levels following inflammasome activation. Similarly, the emodin-induced reduction in the levels of pro-inflammatory cytokines has been reported in other studies (Gao et al., 2021a). Moreover, NO can regulate many physiological processes, such as synaptic transmission and immune responses. However, many studies have found that high NO levels induced by inducible nitric oxide synthase (iNOS) are related to the pathogenesis of MS. NO and iNOS expression levels are elevated in EAE, and, given that NO is associated with blood-brain barrier disruption and oligodendrocyte damage, these pathological alterations all exacerbate EAE severity (Smith and Lassmann, 2002). Several studies have reported the relationship between inflammasomes and iNOS and NO and suggested that inhibition of inflammasome activation can attenuate iNOS and NO levels (Liu et al., 2019; Hou et al., 2022). In our study, treatment with emodin restored iNOS and NO production, which is consistent with the effects of emodin treatment seen in other animal models of disease, supporting the therapeutic effects of emodin in EAE rats and the potential involvement of the NLRP3 signaling pathway (Song et al., 2019; Hu et al., 2021). Moreover, released inflammatory cytokines can promote the aggregation and activation of resting microglia, which in turn release inflammatory cytokines, creating a vicious cycle (Wu et al., 2021). Microglia are involved in the progression of MS. Studies have demonstrated that microglia can exert neuroprotective effects under normal circumstances (Yamasaki et al., 2014), but if activated, they can play a role in the pathogenesis of EAE through mechanisms such as inflammatory cytokine release, antigen presentation, and phagocytosis (Dendrou et al., 2015). In our study, we discovered that emodin treatment reduced microglial aggregation and activation in EAE rats and attenuated inflammation levels in BV2 cells, thus resulting in neuroprotective benefits, similar to previous studies (Kim et al., 2009; Park et al., 2016). These findings provide further insight into the pharmacological mechanism of emodin in the treatment of EAE.

SIRT1 is a nuclear and cytoplasmic sirtuin that deacetylates downstream PGC-1α and is involved in many cellular processes (Tang et al., 2017), such as oxidative stress, inflammation, and mitochondrial function (Wang et al., 2022b). Growing evidence has highlighted the protective effects of SIRT1 in several diseases, including those affecting the CNS. For instance, SIRT1 activation alleviates neurodegeneration in Alzheimer's disease (Zhao et al., 2013), and SIRT1 overexpression is protective against EAE (Nimmagadda et al., 2013). Research has found that SIRT1 exerts its neuroprotective effects by reducing the expression of NLRP3 inflammasome components (Liu et al., 2021a; Xia et al., 2021). The classical activation pathway for NLRP3 is Toll-like receptor 4/NF-κB; NF-κB plays an important role in inflammation as a transcription factor that regulates the expression of NLRP3 inflammasome–related components. NF-κB can be regulated by different factors. Studies have found that SIRT1 can act as an upstream regulator of NF-κB activity (Gao et al., 2021b; Zheng et al., 2022b). We observed lower levels of SIRT1 and PGC-1α expression and higher levels of NLRP3 inflammasome component expression in EAE rats compared with those in rats in the EAE + emodin group. However, emodin treatment resulted in increased SIRT1 and PGC-1α levels and alleviation of symptoms in EAE rats. In addition, other studies have reported similar effects of emodin on SIRT1 and PGC-1α (Yang et al., 2016; Gao et al., 2020). These results suggest that emodin may exert neuroprotective effects in EAE by increasing SIRT1 and PGC-1α levels and inhibiting NLRP3 inflammasome activation.

This study had several limitations. Although the NLRP3 signaling pathway is crucial in MS pathogenesis, other signaling pathways are also involved; therefore, further in-depth research is necessary to clarify the role of other signaling pathways in MS. In addition, all rats were sacrificed at the peak of disease (D14), so we did not observe the long-term effects of emodin; this should be investigated in future experiments.

In this study, we established an EAE rat model by immune induction, resulting in inflammatory cell infiltration and demyelination in EAE rats. Our findings suggest that emodin alleviates inflammation and demyelination in an EAE rat model, possibly through the SIRT1/PGC-1α/NLRP3 signaling pathway and the microglia. We also demonstrated emodin-mediated inhibition of microglial activation in BV2 cells. In conclusion, our results show that emodin alleviates signs of disease in EAE rats, providing a sound experimental basis for the therapeutic use of emodin in the clinical treatment of MS patients.

Acknowledgments: *We gratefully thank members of Feng's lab for their intellectual input.*

Author contributions: *Study design: JF, YRC; experiments performance: YRC, ZQB; manuscript preparation: YRC; data collection and statistical analysis: ZQB, LLY; literature search and collection: HYY; manuscript revision: JF. All authors have read and approved the final manuscript.*

Conflicts of interest: *The authors declare that the research was conducted in the absence of any commercial or financial relationships that could be construed as a potential conflict of interest.*

Availability of data and materials: *All data generated or analyzed during this study are included in this published article and its supplementary information files.*

Additional files:

Additional Figure 1: *The two-dimensional structure of emodin.*

Additional Figure 2: *Schematic diagram of the in vivo experimental design.*

Additional Figure 3: *Schematic diagram of the in vitro experimental design.*

Additional Table 1: *The linear dynamic range of the standard curve for enzyme-linked immunoassay quantifications.*

References

Arifin WN, Zahiruddin WM (2017) Sample size calculation in animal studies using resource equation approach. Malays J Med Sci 24:101-105.

Baecher-Allan C, Kaskow BJ, Weiner HL (2018) Multiple sclerosis: mechanisms and immunotherapy. Neuron 97:742-768.

Bai M, Lu C, An L, Gao Q, Xie W, Miao F, Chen X, Pan Y, Wang Q (2020) SIRT1 relieves necrotizing enterocolitis through inactivation of hypoxia-inducible factor (HIF)-1a. Cell Cycle 19:2018-2027.

Barnett J, Chow J, Ives D, Chiou M, Mackenzie R, Osen E, Nguyen B, Tsing S, Bach C, Freire J, et al. (1994) Purification, characterization and selective inhibition of human prostaglandin G/H synthase 1 and 2 expressed in the baculovirus system. Biochim Biophys Acta 1209:130-139.

Berglund R, Guerreiro-Cacais AO, Adzemovic MZ, Zeitelhofer M, Lund H, Ewing E, Ruhrmann S, Nutma E, Parsa R, Thessen-Hedreul M, Amor S, Harris RA, Olsson T, Jagodic M (2020) Microglial autophagy-associated phagocytosis is essential for recovery from neuroinflammation. Sci Immunol 5:eabb5077.

Bhargava P (2021) Targeting metabolism to treat multiple sclerosis. Neural Regen Res 16:502-503.

Borjini N, Fernández M, Giardino L, Calzà L (2016) Cytokine and chemokine alterations in tissue, CSF, and plasma in early presymptomatic phase of experimental allergic encephalomyelitis (EAE), in a rat model of multiple sclerosis. J Neuroinflammation 13:291.

Brown GC, Neher JJ (2010) Inflammatory neurodegeneration and mechanisms of microglial killing of neurons. Mol Neurobiol 41:242-247.

Browne P, Chandraratna D, Angood C, Tremlett H, Baker C, Taylor BV, Thompson AJ (2014) Atlas of multiple sclerosis 2013: a growing global problem with widespread inequity. Neurology 83:1022-1024.

Burm SM, Peferoen LA, Zuiderwijk-Sick EA, Haanstra KG, t Hart BA, van der Valk P, Amor S, Bauer J, Bajramovic JJ (2016) Expression of IL-1β in rhesus EAE and MS lesions is mainly induced in the CNS itself. J Neuroinflammation 13:138.

Correale J, Farez MF (2015) The role of astrocytes in multiple sclerosis progression. Front Neurol 6:180.

D'Amico E, Zanghì A, Avolio C (2022) Injectable versus oral first-line multiple sclerosis therapies: knows and unknowns from observational studies. Neural Regen Res 17:567-568.

Dąbrowska-Bouta B, Strużyńska L, Sidoryk-Węgrzynowicz M, Sulkowski G (2021) Memantine modulates oxidative stress in the rat brain following experimental autoimmune encephalomyelitis. Int J Mol Sci 22:11330.

Dayani L, Dinani MS, Aliomrani M, Hashempour H, Varshosaz J, Taheri A (2022) Immunomodulatory effects of cyclotides isolated from Viola odorata in an experimental autoimmune encephalomyelitis animal model of multiple sclerosis. Mult Scler Relat Disord 64:103958.

Dendrou CA, Fugger L, Friese MA (2015) Immunopathology of multiple sclerosis. Nat Rev Immunol 15:545-558.

Duewell P, Kono H, Rayner KJ, Sirois CM, Vladimer G, Bauernfeind FG, Abela GS, Franchi L, Nuñez G, Schnurr M, Espevik T, Lien E, Fitzgerald KA, Rock KL, Moore KJ, Wright SD, Hornung V, Latz E (2010) NLRP3 inflammasomes are required for atherogenesis and activated by cholesterol crystals. Nature 464:1357-1361.

Ferrari CC, Depino AM, Prada F, Muraro N, Campbell S, Podhajcer O, Perry VH, Anthony DC, Pitossi FJ (2004) Reversible demyelination, blood-brain barrier breakdown, and pronounced neutrophil recruitment induced by chronic IL-1 expression in the brain. Am J Pathol 165:1827-1837.

Filippi M, Bar-Or A, Piehl F, Preziosa P, Solari A, Vukusic S, Rocca MA (2018) Multiple sclerosis. Nat Rev Dis Primers 4:43.

Gao J, Zhang K, Wang Y, Guo R, Liu H, Jia C, Sun X, Wu C, Wang W, Du J, Chen J (2020) A machine learning-driven study indicates emodin improves cardiac hypertrophy by modulation of mitochondrial SIRT3 signaling. Pharmacol Res 155:104739.

Gao LL, Wang ZH, Mu YH, Liu ZL, Pang L (2022) Emodin promotes autophagy and prevents apoptosis in sepsis-associated encephalopathy through activating BDNF/TrkB signaling. Pathobiology 89:135-145.

Gao R, Wang C, Han A, Tian Y, Ren S, Lv W, Chen A, Zhang J (2021a) Emodin improves intestinal health and immunity through modulation of gut microbiota in mice infected by pathogenic Escherichia coli O(1). Animals (Basel) 11:3314.

Gao T, Wang T, Wang Z, Cao J, Dong Y, Chen Y (2021b) Melatonin-mediated MT2 attenuates colitis induced by dextran sodium sulfate via PI3K/AKT/Nrf2/SIRT1/RORα/NF-κB signaling pathways. Int Immunopharmacol 96:107779.

Gibson SA, Benveniste EN (2018) Protein kinase CK2: an emerging regulator of immunity. Trends Immunol 39:82-85.

Govindarajan V, de Rivero Vaccari JP, Keane RW (2020) Role of inflammasomes in multiple sclerosis and their potential as therapeutic targets. J Neuroinflammation 17:260.

Gris D, Ye Z, Iocca HA, Wen H, Craven RR, Gris P, Huang M, Schneider M, Miller SD, Ting JP (2010) NLRP3 plays a critical role in the development of experimental autoimmune encephalomyelitis by mediating Th1 and Th17 responses. J Immunol 185:974-981.
Guo J, Wang J, Guo R, Shao H, Guo L (2022) Pterostilbene protects the optic nerves and retina in a murine model of experimental autoimmune encephalomyelitis via activation of SIRT1 signaling. Neuroscience 487:35-46.
Guo J, Li B, Wang J, Guo R, Tian Y, Song S, Guo L (2021) Protective effect and mechanism of nicotinamide adenine dinucleotide against optic neuritis in mice with experimental autoimmune encephalomyelitis. Int Immunopharmacol 98:107846.
Heneka MT, Kummer MP, Stutz A, Delekate A, Schwartz S, Vieira-Saecker A, Griep A, Axt D, Remus A, Tzeng TC, Gelpi E, Halle A, Korte M, Latz E, Golenbock DT (2013) NLRP3 is activated in Alzheimer's disease and contributes to pathology in APP/PS1 mice. Nature 493:674-678.
Hou L, Ye Y, Gou H, Tang H, Zhou Y, Xu X, Xu Y (2022) A20 inhibits periodontal bone resorption and NLRP3-mediated M1 macrophage polarization. Exp Cell Res 418:113264.
Hu H, Song X, Li Y, Ma T, Bai H, Zhao M, Wang X, Liu L, Gao L (2021) Emodin protects knee joint cartilage in rats through anti-matrix degradation pathway: An in vitro and in vivo study. Life Sci 269:119001.
Huang J, Khademi M, Fugger L, Lindhe Ö, Novakova L, Axelsson M, Malmeström C, Constantinescu C, Lycke J, Piehl F, Olsson T, Kockum I (2020) Inflammation-related plasma and CSF biomarkers for multiple sclerosis. Proc Natl Acad Sci U S A 117:12952-12960.
Jia C, Zhang J, Chen H, Zhuge Y, Chen H, Qian F, Zhou K, Niu C, Wang F, Qiu H, Wang Z, Xiao J, Rong X, Chu M (2019) Endothelial cell pyroptosis plays an important role in Kawasaki disease via HMGB1/RAGE/cathespin B signaling pathway and NLRP3 inflammasome activation. Cell Death Dis 10:778.
Karussis D (2014) The diagnosis of multiple sclerosis and the various related demyelinating syndromes: a critical review. J Autoimmun 48-49:134-142.
Kim SF, Huri DA, Snyder SH (2005) Inducible nitric oxide synthase binds, S-nitrosylates, and activates cyclooxygenase-2. Science 310:1966-1970.
Kim SH, Jang SD, Lee KY, Sung SH, Kim YC (2009) Chemical constituents isolated from Polygala japonica leaves and their inhibitory effect on nitric oxide production in vitro. J Enzyme Inhib Med Chem 24:230-233.
Kobelt G, Thompson A, Berg J, Gannedahl M, Eriksson J (2017) New insights into the burden and costs of multiple sclerosis in Europe. Mult Scler 23:1123-1136.
Krysko KM, Graves JS, Dobson R, Altintas A, Amato MP, Bernard J, Bonavita S, Bove R, Cavalla P, Clerico M, Corona T, Doshi A, Fragoso Y, Jacobs D, Jokubaitis V, Landi D, Llamosa G, Longbrake EE, Maillart E, Marta M, et al. (2020) Sex effects across the lifespan in women with multiple sclerosis. Ther Adv Neurol Disord 13:1756286420936166.
Lai C, Chen Q, Ding Y, Liu H, Tang Z (2020) Emodin protected against synaptic impairment and oxidative stress induced by fluoride in SH-SY5Y cells by modulating ERK1/2/Nrf2/HO-1 pathway. Environ Toxicol 35:922-929.
Lassmann H (2018) Multiple sclerosis pathology. Cold Spring Harb Perspect Med 8:a028936.
Lassmann H, Bradl M (2017) Multiple sclerosis: experimental models and reality. Acta Neuropathol 133:223-244.
Latz E, Xiao TS, Stutz A (2013) Activation and regulation of the inflammasomes. Nat Rev Immunol 13:397-411.
Li C, Lin H, He H, Ma M, Jiang W, Zhou R (2022) Inhibition of the NLRP3 inflammasome activation by manoalide ameliorates experimental autoimmune encephalomyelitis Pathogenesis. Front Cell Dev Biol 10:822236.
Li Z, Liu F, He X, Yang X, Shan F, Feng J (2019) Exosomes derived from mesenchymal stem cells attenuate inflammation and demyelination of the central nervous system in EAE rats by regulating the polarization of microglia. Int Immunopharmacol 67:268-280.
Liu F, Li Z, He X, Yu H, Feng J (2019) Ghrelin attenuates neuroinflammation and demyelination in experimental autoimmune encephalomyelitis involving NLRP3 inflammasome signaling pathway and pyroptosis. Front Pharmacol 10:1320.
Liu FJ, Gu TJ, Wei DY (2022a) Emodin alleviates sepsis-mediated lung injury via inhibition and reduction of NF-kB and HMGB1 pathways mediated by SIRT1. Kaohsiung J Med Sci 38:253-260.
Liu Y, Shang L, Zhou J, Pan G, Zhou F, Yang S (2022b) Emodin attenuates LPS-induced acute lung injury by inhibiting NLRP3 inflammasome-dependent pyroptosis signaling pathway in vitro and in vivo. Inflammation 45:753-767.
Liu Y, Fan H, Li X, Liu J, Qu X, Wu X, Liu M, Liu Z, Yao R (2021a) Trpv4 regulates Nlrp3 inflammasome via SIRT1/PGC-1α pathway in a cuprizone-induced mouse model of demyelination. Exp Neurol 337:113593.
Liu Z, Yao X, Sun B, Jiang W, Liao C, Dai X, Chen Y, Chen J, Ding R (2021b) Pretreatment with kaempferol attenuates microglia-mediate neuroinflammation by inhibiting MAPKs-NF-κB signaling pathway and pyroptosis after secondary spinal cord injury. Free Radic Biol Med 168:142-154.
Livak KJ, Schmittgen TD (2001) Analysis of relative gene expression data using real-time quantitative PCR and the 2(-Delta Delta C(T)) Method. Methods 25:402-408.
Luo S, Deng X, Liu Q, Pan Z, Zhao Z, Zhou L, Luo X (2018) Emodin ameliorates ulcerative colitis by the flagellin-TLR5 dependent pathway in mice. Int Immunopharmacol 59:269-275.
Mallucci G, Peruzzotti-Jametti L, Bernstock JD, Pluchino S (2015) The role of immune cells, glia and neurons in white and gray matter pathology in multiple sclerosis. Prog Neurobiol 127-128:1-22.
McKenzie BA, Mamik MK, Saito LB, Boghozian R, Monaco MC, Major EO, Lu JQ, Branton WG, Power C (2018) Caspase-1 inhibition prevents glial inflammasome activation and pyroptosis in models of multiple sclerosis. Proc Natl Acad Sci U S A 115:E6065-E6074.
Mei H, Tao Y, Zhang T, Qi F (2020) Emodin alleviates LPS-induced inflammatory response in lung injury rat by affecting the function of granulocytes. J Inflamm (Lond) 17:26.
Mitra S, Anjum J, Muni M, Das R, Rauf A, Islam F, Bin Emran T, Semwal P, Hemeg HA, Alhumaydhi FA, Wilairatana P (2022) Exploring the journey of emodin as a potential neuroprotective agent: novel therapeutic insights with molecular mechanism of action. Biomed Pharmacother 149:112877.
Mohamed DAW, Selim HM, Elmazny A, Genena A, Nabil MM (2022) Apoptotic protease activating factor-1 gene and MicroRNA-484: A possible interplay in relapsing remitting multiple sclerosis. Mult Scler Relat Disord 58:103502.
National Institutes of Health (2011) Guide for the Care and Use of Laboratory Animals, 8th edition. Washington, DC, USA: National Academies Press.
Neyrinck AM, Etxeberria U, Taminiau B, Daube G, Van Hul M, Everard A, Cani PD, Bindels LB, Delzenne NM (2017) Rhubarb extract prevents hepatic inflammation induced by acute alcohol intake, an effect related to the modulation of the gut microbiota. Mol Nutr Food Res 61:1500899.
Nimmagadda VK, Bever CT, Vattikunta NR, Talat S, Ahmad V, Nagalla NK, Trisler D, Judge SI, Royal W, 3rd, Chandrasekaran K, Russell JW, Makar TK (2013) Overexpression of SIRT1 protein in neurons protects against experimental autoimmune encephalomyelitis through activation of multiple SIRT1 targets. J Immunol 190:4595-4607.
Olsson T, Barcellos LF, Alfredsson L (2017) Interactions between genetic, lifestyle and environmental risk factors for multiple sclerosis. Nat Rev Neurol 13:25-36.
Packialakshmi B, Hira S, Lund K, Zhang AH, Halterman J, Feng Y, Scott DW, Lees JR, Zhou X (2022) NFAT5 contributes to the pathogenesis of experimental autoimmune encephalomyelitis (EAE) and decrease of T regulatory cells in female mice. Cell Immunol 375:104515.
Park JE, Lee H, Rho H, Hong SM, Kim SY, Lim Y (2020) Effect of Quamoclit angulata extract supplementation on oxidative stress and inflammation on hyperglycemia-induced renal damage in type 2 diabetic mice. Antioxidants (Basel) 9:459.
Park SY, Jin ML, Ko MJ, Park G, Choi YW (2016) Anti-neuroinflammatory effect of emodin in LPS-stimulated microglia: involvement of AMPK/Nrf2 activation. Neurochem Res 41:2981-2992.
Pilipović I, Stojić-Vukanić Z, Prijić I, Jasnić N, Leposavić G (2020) Propranolol diminished severity of rat EAE by enhancing immunoregulatory/protective properties of spinal cord microglia. Neurobiol Dis 134:104665.
Planavila A, Iglesias R, Giralt M, Villarroya F (2011) Sirt1 acts in association with PPARα to protect the heart from hypertrophy, metabolic dysregulation, and inflammation. Cardiovasc Res 90:276-284.
Schneider CA, Rasband WS, Eliceiri KW (2012) NIH Image to ImageJ: 25 years of image analysis. Nat Methods 9:671-675.
Shen P, Han L, Chen G, Cheng Z, Liu Q (2022) Emodin attenuates acetaminophen-induced hepatotoxicity via the cGAS-STING pathway. Inflammation 45:74-87.
Smith KJ, Lassmann H (2002) The role of nitric oxide in multiple sclerosis. Lancet Neurol 1:232-241.
Song Y, Cui X, Zhao R, Hu L, Li Y, Liu C (2019) Emodin protects against lipopolysaccharide-induced inflammatory injury in HaCaT cells through upregulation of miR-21. Artif Cells Nanomed Biotechnol 47:2654-2661.
Tang S, Fang Y, Huang G, Xu X, Padilla-Banks E, Fan W, Xu Q, Sanderson SM, Foley JF, Dowdy S, McBurney MW, Fargo DC, Williams CJ, Locasale JW, Guan Z, Li X (2017) Methionine metabolism is essential for SIRT1-regulated mouse embryonic stem cell maintenance and embryonic development. EMBO J 36:3175-3193.
Tintore M, Vidal-Jordana A, Sastre-Garriga J (2019) Treatment of multiple sclerosis- success from bench to bedside. Nat Rev Neurol 15:53-58.
Trapp BD, Peterson J, Ransohoff RM, Rudick R, Mörk S, Bö L (1998) Axonal transection in the lesions of multiple sclerosis. N Engl J Med 338:278-285.
Urban JL, Kumar V, Kono DH, Gomez C, Horvath SJ, Clayton J, Ando DG, Sercarz EE, Hood L (1988) Restricted use of T cell receptor V genes in murine autoimmune encephalomyelitis raises possibilities for antibody therapy. Cell 54:577-592.
Walsh JG, Muruve DA, Power C (2014) Inflammasomes in the CNS. Nat Rev Neurosci 15:84-97.
Wang J, Song X, Tan G, Sun P, Guo L, Zhang N, Wang J, Li B (2021a) NAD+ improved experimental autoimmune encephalomyelitis by regulating SIRT1 to inhibit PI3K/Akt/mTOR signaling pathway. Aging (Albany NY) 13:25931-25943.
Wang J, Huangfu M, Li X, Han M, Liu G, Yu D, Zhou L, Dou T, Liu Y, Guan X, Wei R, Chen X (2022a) Osthole induces apoptosis and caspase-3/GSDME-dependent pyroptosis via NQO1-mediated ROS generation in HeLa cells. Oxid Med Cell Longev 2022:8585598.
Wang R, Wu Y, Liu R, Liu M, Li Q, Ba Y, Huang H (2022b) Deciphering therapeutic options for neurodegenerative diseases: insights from SIRT1. J Mol Med (Berl) 100:537-553.
Wang T, Wang J, Sun T, Li Y (2021b) Amelioration of Juglanin against LPS-induced activation of NLRP3 inflammasome in chondrocytes mediated by SIRT1. Inflammation 44:1119-1129.
Wang Y, Zhu W, Lu D, Zhang C, Wang Y (2021c) Tetrahydropalmatine attenuates MSU crystal-induced gouty arthritis by inhibiting ROS-mediated NLRP3 inflammasome activation. Int Immunopharmacol 100:108107.
Wu AG, Zhou XG, Qiao G, Yu L, Tang Y, Yan L, Qiu WQ, Pan R, Yu CL, Law BY, Qin DL, Wu JM (2021) Targeting microglial autophagic degradation in NLRP3 inflammasome-mediated neurodegenerative diseases. Ageing Res Rev 65:101202.
Xia DY, Yuan JL, Jiang XC, Qi M, Lai NS, Wu LY, Zhang XS (2021) SIRT1 promotes M2 microglia polarization via reducing ROS-mediated NLRP3 inflammasome signaling after subarachnoid hemorrhage. Front Immunol 12:770744.
Yamasaki R, Lu H, Butovsky O, Ohno N, Rietsch AM, Cialic R, Wu PM, Doykan CE, Lin J, Cotleur AC, Kidd G, Zorlu MM, Sun N, Hu W, Liu L, Lee JC, Taylor SE, Uehlein L, Dixon D, Gu J, et al. (2014) Differential roles of microglia and monocytes in the inflamed central nervous system. J Exp Med 211:1533-1549.
Yang T, Wang J, Pang Y, Dang X, Ren H, Liu Y, Chen M, Shang D (2016) Emodin suppresses silica-induced lung fibrosis by promoting Sirt1 signaling via direct contact. Mol Med Rep 14:4643-4649.
Yang Y, Liu Y, Wang Y, Chao Y, Zhang J, Jia Y, Tie J, Hu D (2022) Regulation of SIRT1 and its roles in inflammation. Front Immunol 13:831168.
Ye B, Chen X, Dai S, Han J, Liang X, Lin S, Cai X, Huang Z, Huang W (2019) Emodin alleviates myocardial ischemia/reperfusion injury by inhibiting gasdermin D-mediated pyroptosis in cardiomyocytes. Drug Des Devel Ther 13:975-990.
Yeung F, Hoberg JE, Ramsey CS, Keller MD, Jones DR, Frye RA, Mayo MW (2004) Modulation of NF-kappaB-dependent transcription and cell survival by the SIRT1 deacetylase. EMBO J 23:2369-2380.
Zeng P, Shi Y, Wang XM, Lin L, Du YJ, Tang N, Wang Q, Fang YY, Wang JZ, Zhou XW, Lu Y, Tian Q (2019) Emodin rescued hyperhomocysteinemia-induced dementia and Alzheimer's disease-like features in rats. Int J Neuropsychopharmacol 22:57-70.
Zhang M, Li Y, Guo Y, Xu J (2021) Arginine regulates NLRP3 inflammasome activation through SIRT1 in vascular endothelial cells. Inflammation 44:1370-1380.
Zhang Y, Yin K, Wang D, Wang Y, Lu H, Zhao H, Xing M (2022) Polystyrene microplastics-induced cardiotoxicity in chickens via the ROS-driven NF-κB-NLRP3-GSDMD and AMPK-PGC-1α axes. Sci Total Environ 840:156727.
Zhao YN, Li WF, Li F, Zhang Z, Dai YD, Xu AL, Qi C, Gao JM, Gao J (2013) Resveratrol improves learning and memory in normally aged mice through microRNA-CREB pathway. Biochem Biophys Res Commun 435:597-602.
Zheng K, Lv B, Wu L, Wang C, Xu H, Li X, Wu Z, Zhao Y, Zheng Z (2022a) Protecting effect of emodin in experimental autoimmune encephalomyelitis mice by inhibiting microglia activation and inflammation via Myd88/PI3K/Akt/NF-κB signalling pathway. Bioengineered 13:9322-9344.
Zheng Q, Li S, Li X, Liu R (2021) Advances in the study of emodin: an update on pharmacological properties and mechanistic basis. Chin Med 16:102.
Zheng Y, Li L, Chen B, Fang Y, Lin W, Zhang T, Feng X, Tao X, Wu Y, Fu X, Lin Z (2022b) Chlorogenic acid exerts neuroprotective effect against hypoxia-ischemia brain injury in neonatal rats by activating Sirt1 to regulate the Nrf2-NF-κB signaling pathway. Cell Commun Signal 20:84.
Zhu M, Yuan K, Lu Q, Zhu Q, Zhang S, Li X, Zhao L, Wang H, Luo G, Wang T, Huang G, Xu A (2019) Emodin ameliorates rheumatoid arthritis by promoting neutrophil apoptosis and inhibiting neutrophil extracellular trap formation. Mol Immunol 112:188-197.

C-Editor: Zhao M; S-Editors: Yu J, Li CH; L-Editors: Crow E, Yu J, Song LP; T-Editor: Jia Y

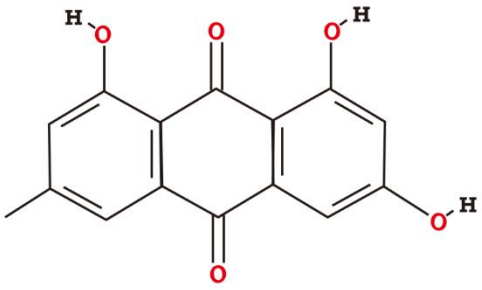

Additional Figure 1 The two-dimensional structure of emodin.

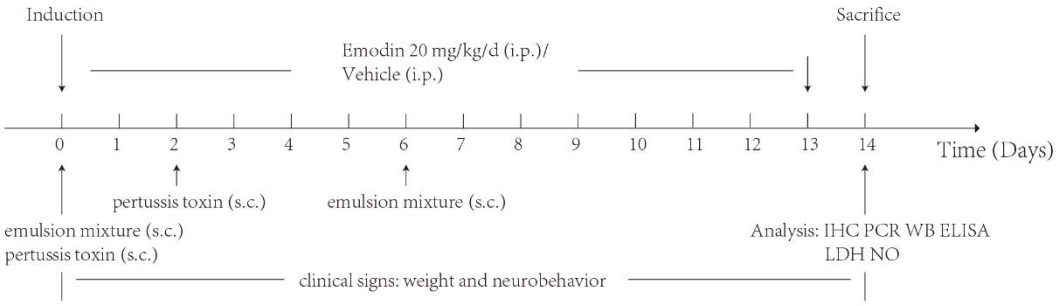

Additional Figure 2 Schematic diagram of the *in vivo* experimental design.

ELISA: Enzyme-linked immunoassay; i.p.: intraperitoneal injection; IHC: immunohistochemistry; LDH: lactate dehydrogenase; NO: nitric oxide; PCR: real-time polymerase chain reaction; s.c.: subcutaneous injection; WB: western blot.

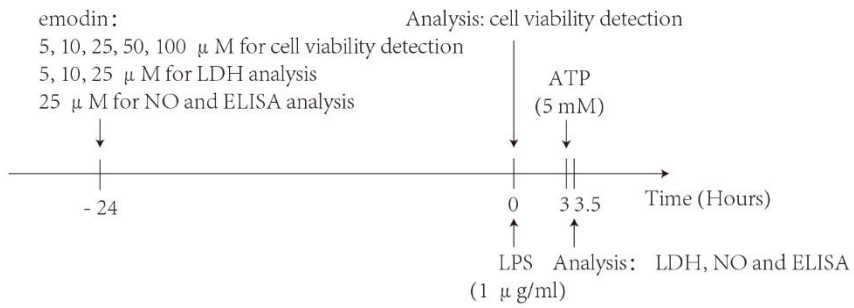

Additional Figure 3 Schematic diagram of the *in vitro* experimental design.

ATP: Adenosine triphosphate; ELISA: enzyme-linked immunoassay; LDH: lactate dehydrogenase; LPS: lipopolysaccharide; NO: nitric oxide.

Additional Table 1 The linear dynamic range of the standard curve for enzyme-linked immunoassay quantifications

In vivo/in vitro	**Antibody**	**Linear dynamic range**
In vivo	TNF-α	10–320 pg/mL
	IL-6	5–160 pg/mL
	IL-1β	1.25–40 pg/mL
	IL-18	5–160 pg/mL
In vitro	TNF-α	20–640 pg/mL
	IL-10	12.5–400 pg/mL
	Arg-1	5–160 μM

Arg-1: Arginase-1; IL-10: interleukin-10; IL-18: interleukin-18; IL-1β: interleukin-1β; IL-6: interleukin-6; TNF-α: tumor necrosis factor-α.